The Emission of Galaxies over the Whole Electromagnetic Spectrum

Denis Burgarella[1], Médéric Boquien[2], Yannick Roehlly[1],
Laure Ciesla[3] and Véronique Buat[1]

1. Aix Marseille Université, CNRS, LAM (Laboratoire d'Astrophysique de Marseille) UMR 7326, 13388, Marseille, France
2. Unidad de Astronomía, Fac. de Ciencias Básicas, Universidad de Antofagasta, Avda. U. de Antofagasta 02800, Antofagasta, Chile
3. Laboratoire AIM-Paris-Saclay, CEA/DSM/Irfu, CNRS, Université Paris Diderot, Saclay, 91191, Gif-sur-Yvette, France

The Spectral Energy Distributions (SEDs) of galaxies contain a wealth of information on the physical processes at play in galaxies and on their components: gas, stars, dust, Active Galactic Nuclei (AGN). Many of the fundamental properties which shape stellar population ensembles are encoded in their SEDs. In this paper, we will try to keep track of the main properties, e.g. star formation history, total mass in stars, characteristics of the AGN, but also the physical state and amount of gas and dust. We will also see how to use modern tools to collect information on the source of the emission in a way consistent with the observed data from the observed far-ultraviolet to far-infrared ranges.

1 Introduction

Galaxies are the bricks of the universe. In themselves, they contain an imprint of the history of the universe. Like any other astrophysical object containing baryonic matter, galaxies emit light over the entire electromagnetic spectrum. Understanding this emission means that we can get a handle on the associated physical processes. It has become clear that addressing the question of the formation and evolution of galaxies in a cosmological context implies that we understand their emission over the broadest electromagnetic spectrum, in contrast to single-wavelength studies which provide us with a far more restricted view. For instance, far-infrared (FIR) data are mandatory if we wish to estimate the star formation rate density at $z < 4$ — the FIR traces dust-absorbed star formation — because the FIR contribution to the total star formation density can reach up to 90% below this redshift (Takeuchi et al., 2005; Burgarella et al., 2013). The first attempts at using multi-wavelength information used correlations of measurements in two bands, e.g. far-ultraviolet (FUV) and FIR, to constrain the dust characteristics or colors, e.g., $FUV - B$ for the stellar ages and masses. Of course, this approach is still valid and we still learn about the galaxies. Nevertheless, modern codes running on ever more powerful computers permit a deeper analysis by combining all the observed spectral energy distribution (SED) to models in just a single step. This SED modelling has now reached a level where tens to hundreds thousands galaxies can be individually compared to tens to

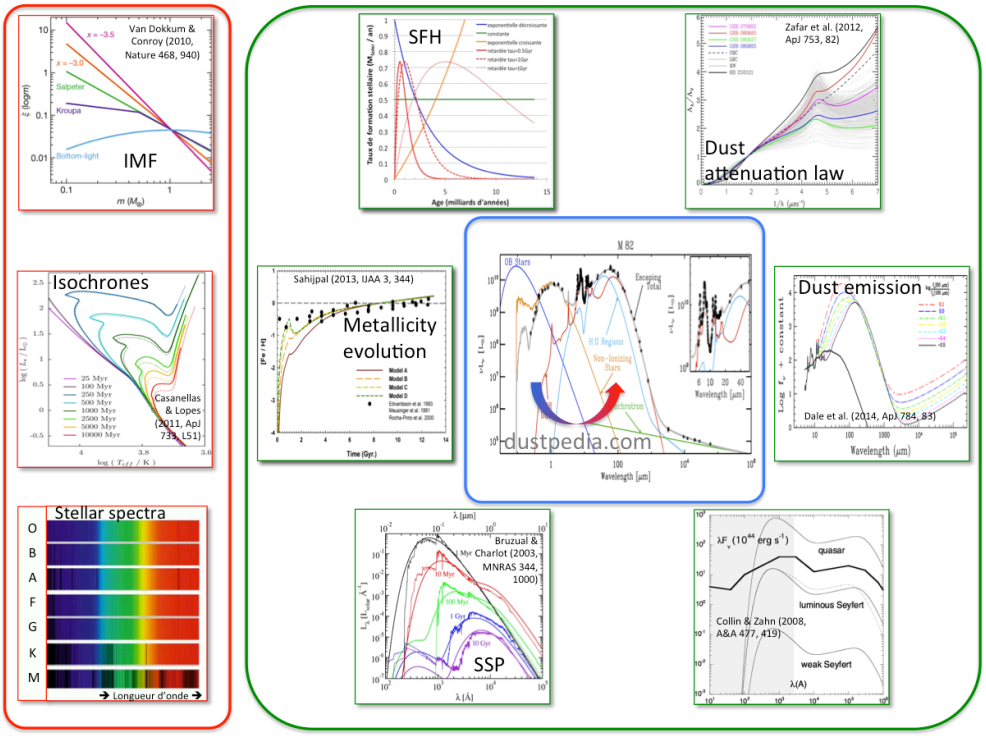

Fig. 1: Most physical processes at play in a galaxy contribute to the shape of the emitted SED, as shown in this figure which makes use of results from van Dokkum & Conroy (2010), Casanellas & Lopes (2011), Zafar et al. (2012), Sahijpal (2013), Bruzual & Charlot (2003), Collin & Zahn (2008) and Dale et al. (2014) and an SED from `http://dustpedia.com`.

hundreds millions of models to obtain not only the best match but also to explore all the models compatible with a given SED, in a statistical way.

2 What information comprises the main ingredients to build a model Spectral Energy Distribution?

Most physical processes have an effect on the observed SED (Fig. 1). However, both the wavelength range and the strength of the effect can vary. For instance, the emission of an Active Galactic Nucleus (AGN) in a Seyfert 2 galaxy can strongly modify the SED in the mid-infrared but hardly in the far-infrared (Hatziminaoglou et al., 2010).

3 What information can be extracted from the Spectral Energy Distribution?

In principle, the information related to the nature of a source is encoded into its SED. However, in practice we must deal with strong limits in deciphering SEDs.

We can easily understand that the quality of the observed SED is at the origin of

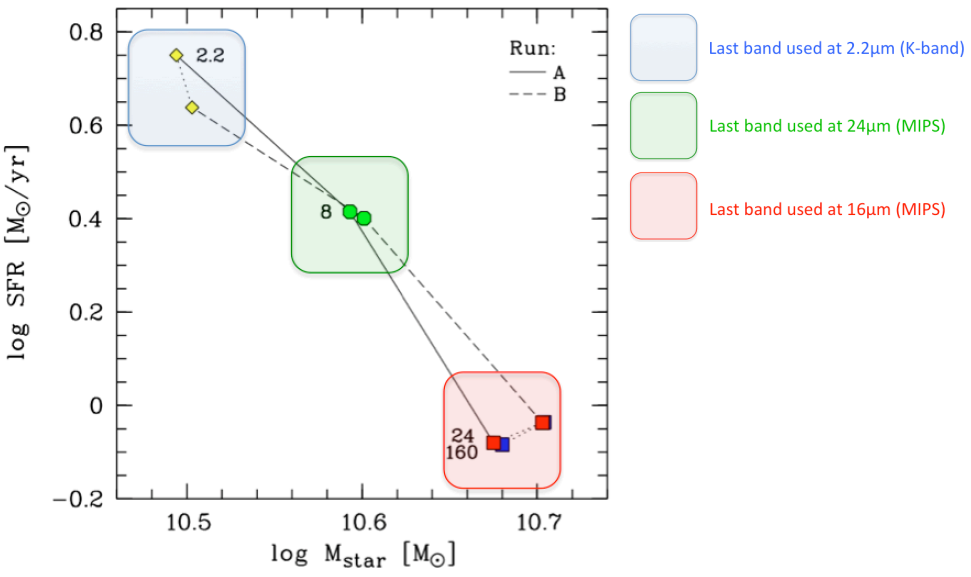

Fig. 2: This figure, extracted from Noll et al. (2009) who fitted the SINGS galaxy sample, shows how restricting the set of filters used in the fit to increasingly fewer infrared leads to a change in the output stellar mass M_{star} and SFR.

one of these limits: if data collected in part of the wavelength have low signal-to-noise ratio, it will be difficult to extract information securely. For instance, estimating the total star formation rate (SFR) of galaxies requires good-quality data in the wavelength range corresponding to dust emission at tens to hundreds of Kelvins, that is, in the rest-frame mid- to far-infrared (Fig. 2). However, collecting far-infrared data can be a difficult challenge for intrinsically-faint nearby objects or for bright but distant objects. Without reliable infrared data, crucial parameters such as the dust mass or the dust temperature cannot be safely inferred. Even the amount of dust attenuation can be a problem: we can use, e.g., the slope of the ultraviolet spectrum or the stellar mass to obtain an estimate of the dust attenuation (A_V or A_{FUV}).

Besides, even when relatively good data are available, we might face degeneracies when using broad-band SEDs. For instance, the reddening of the ultraviolet-optical spectrum can be due to dust and/or to the age of the stellar populations. With the help of far-infrared data, we can remove or at least reduce this degeneracy by using redundant information on the dust attenuation, which means that we can, to some extent, hope to decouple the effects of dust attenuation from that of the age on the ultraviolet-optical spectrum.

In conclusion, it is wise when performing any SED modelling to be able to estimate the uncertainties on the physical parameters. However, beyond these uncertainties, it is even wiser to control the number of degeneracies by carrying out tests on a mock catalogue built to be not too far from the observed data, and for which we have full knowledge (as best as we can from a model) of the parameters we are trying to estimate Giovannoli et al. (2011). These tests allow us to compare the input and output values of the physical parameters and quantitatively evaluate our capacity to

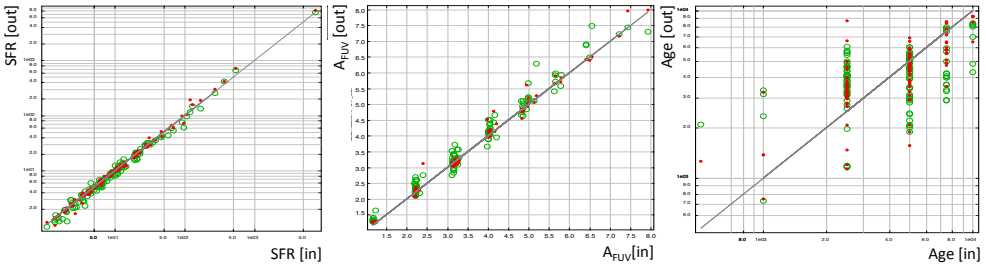

Fig. 3: Building mock catalogues, as shown in this mosaic from the SED modelling code *CIGALE*, allows evaluation of the quality of the parameter estimation process. Here, for instance, the SFR (left) outputs from CIGALE correlate with the SFR inputs: we can conclude that we have a good estimate of their true value. For the FUV dust attenuation (centre), the comparison is still good and we deduce that we have a good handle on the amount of dust attenuation in the FUV. This parameter, of course, plays a crucial role in the estimated SFR. However, we notice that, for this dataset and this fit, the information that we can get on the age of the stellar population is imprecise and we cannot safely use the ages estimated. In this mosaic, red and green points are related to two different star formation histories).

estimate them and, sometimes, even estimate the range over which we can trust our results (Fig. 3).

4 Two generic types of SED modelling codes

In this section, we will present two different types of codes that allow modelling of SEDs and fitting observed SEDs.

4.1 Radiative Transfer codes

In the presence of dust grains in the environment around stars, the emission of the stellar radiation is scattered, absorbed and re-emitted by dust. That is what we refer to when we mention the dust attenuation. The spectrum emerging from this circumstellar processing provides the astronomer with the only available information about the embedded stellar populations.

Radiative Transfer codes model the transport of radiation in these dusty circumstellar environments by making assumptions about important parameters such as the chemical composition, the star formation history, and the dust/star geometry of galaxies. These codes solve the radiation transport equation coupled self-consistently with the equation of motion for the outflow of gas and dust grains. They include the properties for the most common types of astronomical dust and support various analytical forms for the density distribution in galaxies.

Among the main phases in building the modelled SEDs, the specification of geometry is an important one. This means that the user must specify the distributions of stars and dust, both at different scales in the modelled galaxy. This is therefore a fundamental step before actually running the radiative transfer calculations to derive the radiation fields in galaxies, which will permit evaluation of the temperature

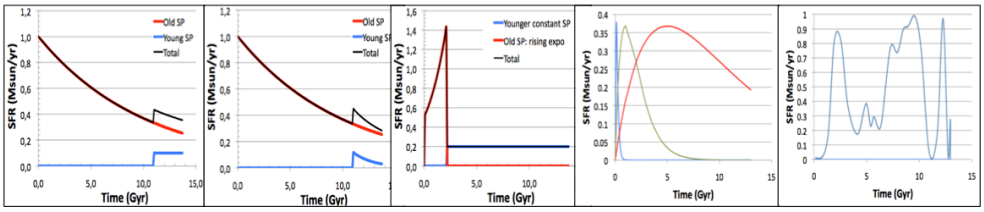

Fig. 4: Among other hypotheses, the output SED is constrained by the input star formation history. The code *CIGALE* in its new Python version is very modular and allows use of a wide range of star formation histories. Examples are shown here from left to right: declining exponential plus late constant burst, declining exponential plus exponential burst, increasing exponential plus constant burst, different delayed histories controlled by τ parameters and finally any history given in an input table provided, e.g., by semi-analytical models or hydrodynamical simulations (e.g.Boquien et al. (2014)). The modularity of *CIGALE* easily allows creation of new analytical star formation histories.

distribution of grains of different sizes and composition as a function of position in the galaxy. Finally, by integrating over all positions in a given galaxy, we obtain the modelled SED (e.g., Popescu et al. (2011), Baes et al. (2011), Silva (2009), Efstathiou et al. (2013)).

4.2 Phenomenological codes with energy balance: the CIGALE example.

Several phenomenological codes use the energy balance to model SEDs and fit observed ones (*MagPhys*: da Cunha et al. (2008), *CIGALE*: Noll et al. (2009), Burgarella et al. (2016, in prep.) and Boquien et al. (2016 in prep.)). In the rest of this section, we will more specifically present *CIGALE* [1].

Phenomenological codes use a different philosophy from radiative transfer codes. They model the various phenomena which contribute to the total galaxy SED and combine them to produce a global modelled SED. The first phase consists of assuming a star formation history. Several options are available depending on which code is used.

In the code *CIGALE* (Code Investigating the GALaxy Emission), a wide range of analytical star formation histories can be used (constant, exponentially increasing or declining, delayed, periodic, etc.), but it is also possible to use a table describing the time evolution of the star formation history that might be, e.g., an output from semi-analytical models (Fig. 4)

In the next phase, we define which Simple Stellar Population (SSP) model is chosen for this run. *CIGALE* provides a choice between Maraston (2005) and Bruzual & Charlot (2003) in the public version. Once the SSP is selected, it is combined with the star formation history to obtain the dust-free emission of the complex stellar population, i.e., a galaxy. In the presence of dust, we have to account for the dust attenuation. In *CIGALE*, we offer the possibility of having parametric dust attenuation laws where the basis is the Calzetti law. However, since we know that this law is not valid for all galaxies, we can modify the slope and/or add a bump at 217.5 nm (see Eq. 1) as described in Buat et al. (2012):

[1] http://cigale.lam.fr

$$\frac{A(\lambda)}{E_{B-V}} = \left[k(\lambda) \times \left(\frac{\lambda}{5500\text{Å}}\right)^{\delta}\right] + \left[\frac{E_{bump}\lambda^2\gamma^2}{(\lambda^2-\lambda_0)^2+\lambda^2\gamma^2}\right], \quad (1)$$

where $k(\lambda)$ is the composite dust attenuation law from Leitherer et al. (2002) below 150 nm and by Calzetti et al. (2000) above 150 nm. Since young and old stars do not suffer from the same amount of dust attenuation, it is possible to constrain the ratio $E_{old}(B-V)/E_{young}(B-V)$ in *CIGALE*.

As in any energy balance model, *CIGALE* assumes that all the energy processed by dust is re-emitted in the infrared. The shape of the emission is provided by one of several options. In the public version Draine & Li (2007), Dale et al. (2014) and Casey (2012) are available at the moment.

The nebular emission (continuum and lines) is also computed from the ultraviolet to the near-infrared (if requested). Given the number of Lyman continuum photons, *CIGALE* computes the Hβ line luminosity and, then the other lines using the metallicity and radiation field intensity dependent templates that provide the ratio between individual lines and Hβ (Inoue, 2011). The nebular continuum is scaled directly from the number of ionizing photons.

Emission from an AGN can finally be added using, e.g. Fritz et al. (2006) models. For a detailed description of fitting SEDs using an AGN model, we refer to Ciesla et al. (2015).

Finally, the last and mandatory module in CIGALE redshifts the modelled SEDs and add the absorption from the inter-galactic medium (Meiksin, 2006).

Models can be built without any observed data. However, in this paper we are interested in SED fitting. *CIGALE* uses a statistical approach where it computes the probability distribution function for each object and each analysed parameter. We can estimate the physical parameters associated to any observed SED. It is important to note that *CIGALE* needs a redshift to run. Even though providing a range of redshifts allows estimation of a redshift for an observed SED by comparing the probability that the redshifted SEDs would match the observed one, *CIGALE* is not presently designed to estimate redshifts for large galaxy sample.

Plotting the best model that matches the observed SED (Figs. 4.2 and 4.2) allows checking of the quality of the fit. However, beyond this best model described in the first output file, *CIGALE* provides an output file with the parameters and the associated uncertainties for each galaxy and each analysed parameter.

An optional creation of a mock catalogue from the data and a subsequent SED analysis is finally possible as described above.

Two important features of *CIGALE* are:

1. A SED fitting analysis can be long for very large number of models and/or very large sample of objects. To make runs possible in a reasonable amount of time, *CIGALE* is parallelized and can run on multi-core computers.

2. *CIGALE* is very modular (Fig. 7) and it is easy to add new models, templates, star formation history, dust attenuation laws, etc. by simply adding a new module (with the correct interface) in the appropriate directory.

Acknowledgements. We thank the organizers.

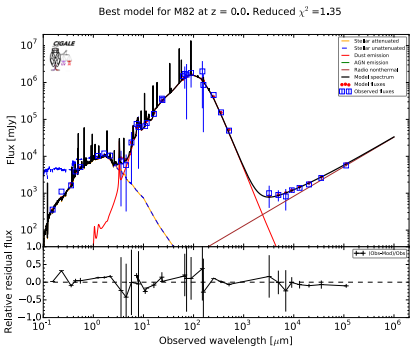

Fig. 5: *CIGALE* best for Messier 82. The blue line is the unattenuated stellar spectrum. The orange line represents the attenuated spectrum. The red line is the dust emission. Note that radio emission is also included for this fit.

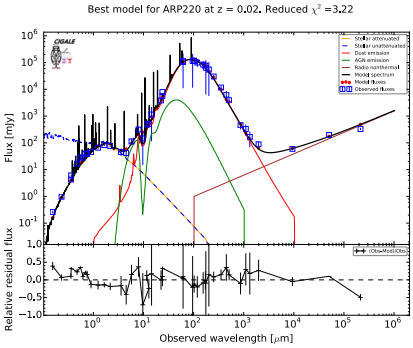

Fig. 6: *CIGALE* best for Arp 220 that also includes (green) AGN emission. In both panels, the lower sub-plot presents the residual relative flux computed as $(f_{observed} - f_{model})/f_{observation}$ in the same wavelength range.

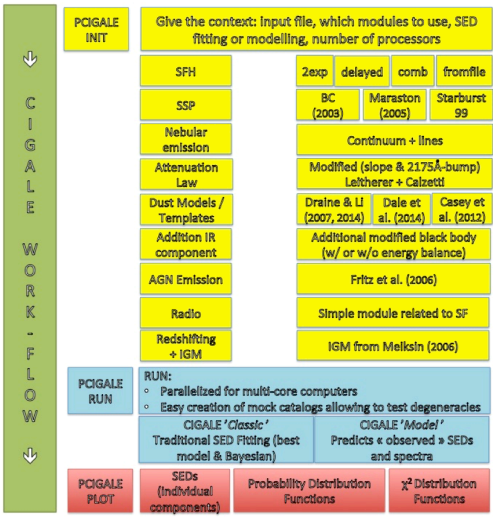

Fig. 7: The modularity of *CIGALE* is illustrated in this flow chart. Any new module can be added to modify or introduce new functionality into *CIGALE*.

References

Baes, M., et al., *Efficient Three-dimensional NLTE Dust Radiative Transfer with SKIRT*, ApJS **196**, 22 (2011), 1108.5056

Boquien, M., Buat, V., Perret, V., *Impact of star formation history on the measurement of star formation rates*, A&A **571**, A72 (2014), 1409.5792

Bruzual, G., Charlot, S., *Stellar population synthesis at the resolution of 2003*, MNRAS **344**, 1000 (2003), astro-ph/0309134

Buat, V., et al., *GOODS-Herschel: dust attenuation properties of UV selected high redshift galaxies*, A&A **545**, A141 (2012), 1207.3528

Burgarella, D., et al., *Herschel PEP/HerMES: the redshift evolution ($0 \leq z \leq 4$) of dust attenuation and of the total (UV+IR) star formation rate density*, A&A **554**, A70 (2013), 1304.7000

Calzetti, D., et al., *The Dust Content and Opacity of Actively Star-forming Galaxies*, ApJ **533**, 682 (2000), astro-ph/9911459

Casanellas, J., Lopes, I., *Signatures of Dark Matter Burning in Nuclear Star Clusters*, ApJ **733**, L51 (2011), 1104.5465

Casey, C. M., *Far-infrared spectral energy distribution fitting for galaxies near and far*, MNRAS **425**, 3094 (2012), 1206.1595

Ciesla, L., et al., *Constraining the properties of AGN host galaxies with spectral energy distribution modelling*, A&A **576**, A10 (2015), 1501.03672

Collin, S., Zahn, J.-P., *Star formation in accretion discs: from the Galactic center to active galactic nuclei*, A&A **477**, 419 (2008), 0709.3772

da Cunha, E., Charlot, S., Elbaz, D., *A simple model to interpret the ultraviolet, optical and infrared emission from galaxies*, MNRAS **388**, 1595 (2008), 0806.1020

Dale, D. A., et al., *A Two-parameter Model for the Infrared/Submillimeter/Radio Spectral Energy Distributions of Galaxies and Active Galactic Nuclei*, ApJ **784**, 83 (2014), 1402.1495

Draine, B. T., Li, A., *Infrared Emission from Interstellar Dust. IV. The Silicate-Graphite-PAH Model in the Post-Spitzer Era*, ApJ **657**, 810 (2007), astro-ph/0608003

Efstathiou, A., Christopher, N., Verma, A., Siebenmorgen, R., *Active galactic nucleus torus models and the puzzling infrared spectrum of IRAS F10214+4724*, MNRAS **436**, 1873 (2013), 1310.0368

Fritz, J., Franceschini, A., Hatziminaoglou, E., *Revisiting the infrared spectra of active galactic nuclei with a new torus emission model*, MNRAS **366**, 767 (2006), astro-ph/0511428

Giovannoli, E., et al., *Population synthesis modelling of luminous infrared galaxies at intermediate redshift*, A&A **525**, A150 (2011), 1006.5555

Hatziminaoglou, E., et al., *HerMES: Far infrared properties of known AGN in the HerMES fields*, A&A **518**, L33 (2010), 1005.2192

Inoue, A. K., *Rest-frame ultraviolet-to-optical spectral characteristics of extremely metal-poor and metal-free galaxies*, MNRAS **415**, 2920 (2011), 1102.5150

Leitherer, C., Li, I.-H., Calzetti, D., Heckman, T. M., *Global Far-Ultraviolet (912-1800 Å) Properties of Star-forming Galaxies*, ApJS **140**, 303 (2002)

Maraston, C., *Evolutionary population synthesis: models, analysis of the ingredients and application to high-z galaxies*, MNRAS **362**, 799 (2005), astro-ph/0410207

Meiksin, A., *Colour corrections for high-redshift objects due to intergalactic attenuation*, MNRAS **365**, 807 (2006), astro-ph/0512435

Noll, S., et al., *Analysis of galaxy spectral energy distributions from far-UV to far-IR with CIGALE: studying a SINGS test sample*, A&A **507**, 1793 (2009), 0909.5439

Popescu, C. C., et al., *Modelling the spectral energy distribution of galaxies. V. The dust and PAH emission SEDs of disk galaxies*, A&A **527**, A109 (2011), 1011.2942

Sahijpal, S., *Influence of Supernova SN Ia Rate and the Early Star Formation Rate on the Galactic Chemical Evolution*, *International Journal of Astronomy and Astrophysics* **3**, 344 (2013)

Silva, L., *Multi-Wavelength Modelling of Dusty Galaxies. GRASIL and Applications*, in Revista Mexicana de Astronomia y Astrofisica Conference Series, *Revista Mexicana de Astronomia y Astrofisica Conference Series*, volume 37, 83–93 (2009)

Takeuchi, T. T., Buat, V., Burgarella, D., *The evolution of the ultraviolet and infrared luminosity densities in the universe at $0 < z < 1$*, A&A **440**, L17 (2005), astro-ph/0508124

van Dokkum, P. G., Conroy, C., *A substantial population of low-mass stars in luminous elliptical galaxies*, Nature **468**, 940 (2010), 1009.5992

Zafar, T., et al., *The Properties of the 2175 Å Extinction Feature Discovered in GRB Afterglows*, ApJ **753**, 82 (2012), 1205.0387